ISSN: 1304-7981 Number: **10**, Year: **2016**, Pages: **01-09** **http://jnrs.gop.edu.tr**

Gaziosmanpasa University
Graduate School of Natural and Applied Sciences
Journal of New Results in Science

Received: 29.08.2015 *Editors-in-Chief*: Bilge Hilal Cadirci
Accepted: 10.12.2015 *Area Editor*: Serkan Demiriz

Effect of Porosity on the Peristaltic Pumping of a Non-Newtonian Fluid in a Channel

G.C.SANKAD [a,1] (math.gurunath@bldeacet.ac.in)
ASHA PATIL[a] (math.asha@bldeacet.ac.in)

[a] VTU Research Center, Department of Mathematics, BLDEA's VP Dr. PGH College of Engg. & Tech. Vijayapur-586 103 (Karnataka)-INDIA

Abstract – The peristaltic flow of a non-Newtonian fluid in a flexible channel, with permeable walls, under the assumptions of long wavelength and low Reynolds number is studied. The pressure rise and frictional force are discussed for various parameters of interest like yield stress, Darcy number etc. through graphs. It is observed that with increase in porosity, there is pressure drop in the pumping region while there is a pressure rise in the co-pumping region. The behavior of the volume flow rate $\bar{Q}$ is similar for both the pressure difference and frictional force, for the variation of all the parameters.

Keywords -
flow, non-Newtonian fluid, Darcy number, pressure rise, frictional force.

1. Introduction

The word peristaltic comes from a Greek word "Peristaltikos" which means clasping and compressing. Thus 'Peristalsis' is the rhythmic sequence of smooth muscle contractions that progressively squeeze one small section of the tract and then the next, to push the content along the tract. It induces propulsion and mixing movements and pumps the content against pressure rise, thus finding enormous physiological, biomedical and industrial applications. The swallowing of food through the esophagus, movement of chyme in the gastrointestinal tract, transport of urine from kidney to the bladder, etc. are some of the physiological applications, mechanical devices like finger pumps, roller pumps are also based on the peristaltic mechanism. It is also speculated that peristalsis may be involved in the translocation of water in tall trees, through its porous matrix.

[1] ***Corresponding Author***

By the mechanical point of view, the peristaltic motion is characterized by the dynamic interaction of flexible boundary with the fluid. Probably Latham [1] was the first to study the peristaltic mechanism which has attracted a large number of researchers towards the study of peristalsis. The experimental results obtained by Latham [1] were found to be in good agreement with the theoretical analysis of Shapiro [2].

Tang and Fung [4] and many authors have considered blood and other biofluids to behave like a Newtonian fluid for physiological peristalsis. Though the Newtonian approach of blood gives satisfactory results for the ureter mechanism, it fails to do so in small blood vessels and intestine. Several models for physiological flows were suggested by Kapur [5] considering blood as both Newtonian and non-Newtonian fluids. The effect of various parameters for the peristaltic transport of a Hyperbolic tangential nanofluid in the presence of a heat source with the combined effects of thermal radiation and internal magnetic field in a tapered asymmetric channel is investigated by Kothandapani and Prakash [9].

The combined effect of partial slip and nanofluid on the peristaltic transport of a Jeffery fluid is studied by Akram and Nadeem [12]. Applying Homotopy perturbation method they have obtained the solution of the coupled nonlinear equations of temperature and nano particle volume fraction.

A porous medium is a material containing pores or spaces between solid material through which liquid or gas can pass. As most of the tissues in the body are deformable porous media, flow through porous media has been of considerable interest, in the recent years, to understand the various medical conditions (viz., tumor growth) and treatments (injections).

The first study of peristaltic flow through a porous medium is presented by Elshahawey et al [6]. The peristaltic flow of Herschel-Bulkley fluid in an inclined channel lined with porous material is studied by Sreenadh et al. [8]. In swallowing the food bolus through the oesophagus, the heat transfer effect and the effect of elasticity of flexible walls with porous medium is studied by Abdulhadi [10], assuming the bolus to be Jeffery fluid. He observed that the size of the trapped bolus increases with an increase in the Jeffery parameter, rigidity and stiffness.

Herschel-Bulkley fluid is considered to be the more general non-Newtonian fluid as it contains two parameters, the yield stress and power law index. Also Herschel-Bulkley fluid’s constitutive equation can be reduced to the constitutive equations of Newtonian, Power law, and Bingham fluid models. Blair and Spanner’s [3] investigations revealed that the Herschel-Bulkley fluid model very closely explains the phenomenon for cow’s blood. Very recently, Santhosh and Radhakrishnamacharya [11] have considered the flow of Herschel-Bulkley fluid through narrow tubes.

As mentioned above, many authors have worked on different non-Newtonian fluids without porosity. Therefore with the purpose of studying the peristaltic transport of a non-Newtonian fluid in a channel with porous lining, we have considered the flow modeled for a Herschel-Bulkley fluid in a uniform flexible channel with porous walls. This helps in the better understanding of the peristaltic pumping of blood in small vessels. The expressions for pressure rise and frictional force are obtained under long wavelength and low Reynolds number. The effects of Darcy number, thickness of the porous lining, yield stress and index on the pressure rise and the frictional force are discussed and depicted through graphs.

2. Mathematical formulation

Consider the flow of a non-Newtonian fluid, obeying Herschel–Bulkley model, in a channel of width '$2a$' lined with non erodible porous material. The flexible wall of the channel is subjected to a progressive peristaltic wave with amplitude b, wave length λ and wave speed c. We restrict the discussion to the half width of the channel as shown in Fig. 1. The region between $y = 0$ and $y = y_0$ is called the plug flow region where $|\tau_{xy}| \leq \tau_0$ and in the region between $y = y_0$ and $y = H$, we have $|\tau_{xy}| \geq \tau_0$.

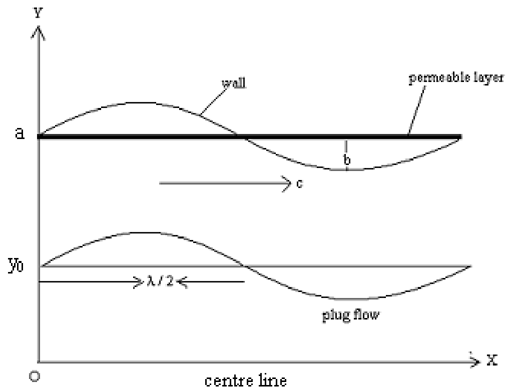

Fig. 1

The wall deformation is given by, $Y = H(X, t) = a + b\sin\frac{2\pi}{\lambda}(X - ct)$ (1)

Let us assume that the flow becomes steady in the wave frame (x, y) [moving with the velocity c away from the laboratory frame (X, Y)] considering the channel length to be an integral multiple of the wavelength λ and also we assume that at the ends of the channel, the pressure difference is constant.

The transformation between these two frames is given by

$$x = X - ct; y = Y;\ u(x,y) = U(X - ct, Y) - c;\ v(x,y) = V(X - ct, Y);\ p(x) = P(X,t),$$

where U,V are velocity components in the laboratory frame and u,v are velocity components in the wave frame. As proved experimentally, the Reynolds number of the flow is very small in many physiological situations. We assume that the flow is inertia free and the wavelength is infinite. The following non-dimensional quantities are used to make the basic equations and the boundary conditions dimensionless.

$$x' = \frac{x}{\lambda};\quad y' = \frac{y}{a};\quad h' = \frac{h}{a};\quad t' = \frac{ct}{\lambda};\quad \epsilon' = \frac{\epsilon}{a};\quad {\tau_0}' = \frac{\tau_0}{\mu(\frac{c}{a}^n)};$$

$$\psi' = \frac{\psi}{ac};\quad q' = \frac{q}{ac};\quad u' = \frac{u}{c};\quad F' = \frac{fa}{\mu\lambda c};\quad \phi = \frac{b}{a};\quad Da = \frac{k}{a^2}.$$

Under the lubrication approach, the governing equations of motion after dropping primes are as follows :

$$\frac{\partial}{\partial y}(\tau_{yx}) = -\frac{\partial p}{\partial x}, \quad (2)$$

Where
$$\tau_{yx} = \left(-\frac{\partial u}{\partial y}\right)^n + \tau_0, \tag{3}$$

and the dimensionless boundary conditions are
$$\psi = 0 \quad \text{at} \quad y = 0\,, \tag{4}$$

$$\psi_{yy} = 0 \quad \text{at} \quad y = 0\,, \tag{5}$$

$$\tau_{yx} = 0 \quad \text{at} \quad y = 0\,, \tag{6}$$

$$u = -\frac{\sqrt{Da}}{\alpha}\frac{\partial u}{\partial y} - 1 \quad \text{at} \ y = h(x) - \epsilon. \tag{7}$$

3. Solution of the problem

On solving equations (2) and (3) together with $u = \frac{\partial \psi}{\partial y}$, $v = -\frac{\partial \psi}{\partial x}$ and the boundary conditions (4) - (7), we obtain the velocity field as

$$u = P^m\left[\frac{1}{m+1}\{(h-\epsilon-y_o)^{m+1} - (y-y_o)^{m+1}\} + \frac{\sqrt{Da}}{\alpha}(h-\epsilon-y_o)^m\right] - 1, \tag{8}$$

where $\quad P = -\frac{\partial p}{\partial x}$ and $m = \frac{1}{n}$, (9)

We find the upper limit of the plug flow region using the boundary condition $\psi_{yy} = 0$ at $y = y_0$, so that we have, $y_0 = \frac{\tau_0}{P}$.

Also $P = \frac{\tau_{h-\epsilon}}{h-\epsilon}$, under the condition $\tau_{xy} = \tau_{h-\epsilon}$ at $y = h - \epsilon$. Therefore, $\frac{y_0}{h-\epsilon} = \frac{\tau_o}{h-\epsilon} = \tau$; $0 < \tau < 1$.

Taking $y = y_o$ in (8), we get the velocity in the plug flow region as

$$u_p = P^m(h-\epsilon-y_o)^m\left(\frac{h-\epsilon-y_o}{1+m} + \frac{\sqrt{Da}}{\propto}\right) - 1, \tag{10}$$

We obtain the stream function, on integrating equations (9) and (10) and using the conditions $\psi_p = 0$ and $\psi = \psi_p$ at $y = y_o$, as

$$\psi = P^m\left[\frac{1}{m+1}\left\{(h-\epsilon-y_o)^{m+1}y - \frac{(y-y_o)^{m+2}}{m+2}\right\} + \frac{\sqrt{Da}}{\alpha}(h-\epsilon-y_0)^m\, y\right] - y, \tag{11}$$

$$\psi_p = \int u_p dy = P^m(h-\epsilon-y_0)^m\left(\frac{h-\epsilon-y_0}{m+1} - \frac{\sqrt{Da}}{\alpha}\right)y - y. \tag{12}$$

The volume flux ‘q’ through each cross section in the wave frame is given by
$$q = \int_0^{y_0} u_p dy + \int_{y_0}^{h-\epsilon} u\, dy$$

$$q = P^m\left[\frac{(h-\epsilon-y_0)^{m+1}}{m+1}\left\{h-\epsilon-\frac{(h-\epsilon-y_0)}{m+2}\right\}+\ (h-\epsilon-y_0)^m\frac{\sqrt{Da}}{\alpha}(h-\epsilon)\right]-(h-\epsilon). \quad (13)$$

From equation (13) we get,

$$P = -\frac{\partial p}{\partial x} = \left[\frac{(q+h-\epsilon)(m+1)(m+2)\alpha}{(h-\epsilon)^{m+1}(1-\tau)^m\{\alpha(h-\epsilon)(1-\tau)\{(m+2)-(1-\tau)\}+\sqrt{Da}(m+1)(m+2)\}}\right]^{\frac{1}{m}}. \quad (14)$$

In the laboratory frame between the central line and the wall the instantaneous volume flow rate $Q(X,t)$ is

$$Q(X,t) = \int_0^H U(X,Y,t)dY. \quad (15)$$

Averaging equation (15) over one period yield the time mean flow (time-averaged volume flow rate) $\bar{Q}$ as,

$$\bar{Q} = \frac{1}{T}\int_0^T Qdt = q+1. \quad (16)$$

The pressure rise over one cycle of the wave is obtained by integrating equation (14) with respect to ‘x’ over one wavelength,

$$\Delta P = \int_0^1 \frac{\partial p}{\partial x}\,dx = -\int_0^1 P\,dx. \quad (17)$$

The dimensionless frictional force F at the wall across one wavelength is given by

$$F = \int_0^1 h\left(-\frac{\partial p}{\partial x}\right)dx. \quad (18)$$

4. Discussion of Results

From equation (17), we have obtained the pressure difference Δp as a function of the volume flow rate $\bar{Q}$, for a Herschel Bulkley fluid. The effects of various parameters are observed with the help of graphs that are obtained using Mathematica software.

Fig 2 shows the pressure difference Δp as a function of the volume flow rate $\bar{Q}$ for different values of Darcy number and for fixed values of τ, n, α *and* ϵ. It is observed that in the pumping region $(\Delta p > 0)$, for a given volume flow rate $\bar{Q}$ the pressure difference decreases with an increase in the Darcy number and for a fixed pressure difference Δp, it is seen that the volume flow rate $\bar{Q}$ decreases with an increase in the Darcy number. For free pumping region $(\Delta p = 0)$, the variation of Darcy number has no effect on $\bar{Q}$. In the co-pumping region $(\Delta p < 0)$, for a given volume flow rate $\bar{Q}$ the pressure difference increases with an increase in the Darcy number and for a fixed pressure difference Δp, as the Darcy number increases, the volume flow rate $\bar{Q}$ also increases.

In Fig.3 we have obtained the pressure difference Δp as a function of the volume flow rate $\bar{Q}$, for different values of τ and for fixed values of other parameters. It is observed that in the pumping region, for a given volume flow rate $\bar{Q}$ the pressure difference increases with an increase in the yield stress τ and for a fixed pressure difference Δp, it is seen that the volume flow rate $\bar{Q}$ also increases as the yield stress increases. For free pumping region there is no effect of τ on $\bar{Q}$. In the co-pumping region, for a given volume flow rate $\bar{Q}$, the pressure difference decreases with an increase in the yield stress and for a fixed pressure difference Δp, the volume flow rate $\bar{Q}$ decreases as the yield stress increases.

The effect of porous thickening ϵ, for fixed $Da, n, \alpha \; and \; \tau$ is shown in Fig. 4. It is seen that in the pumping region, for a given volume flow rate $\bar{Q}$ the pressure difference increases with an increase in the value of ϵ and for a fixed pressure difference Δp, it is seen that the volume flow rate $\bar{Q}$ also increases with an increase in ϵ. In the free pumping region also, volume flow rate $\bar{Q}$ increases with an increase in ϵ. In the co-pumping region, for $0.4 < \bar{Q} < 0.85$, there is no effect of ε on Δp as well on $\bar{Q}$ and for $0.85 < \bar{Q} < 1$, for fixed volume flow rate $\bar{Q}$, Δp decreases as ε increases and for fixed Δp, $\bar{Q}$ decreases slightly for increase in the values of ϵ.

The effect of the index n for fixed values of other parameters $\alpha, \epsilon, \tau \; and \; Da$ is depicted in Fig.5. It is observed that in the pumping region, for a given volume flow rate $\bar{Q}$ the pressure difference decreases with an increase in the index n and for a fixed pressure difference Δp, it is seen that the volume flow rate $\bar{Q}$ also decreases with an increase in the index number. For free pumping region, volume flow rate $\bar{Q}$ decreases with an increase in n. In the co-pumping region, for a given volume flow rate $\bar{Q}$, the pressure difference increases with an increase in n and for a fixed pressure difference Δp, as the index increases, the volume flow rate $\bar{Q}$ also increases.

From equation (18), the Frictional force F is obtained as a function of the volume flow rate $\bar{Q}$, and the effect of various parameters are shown from Fig. 6 – Fig. 9.

Fig. 6 depicts the effect of Darcy number variation, for fixed values of $\tau, n, \alpha \; and \; \epsilon$. It is observed that for a given volume flow rate $\bar{Q}$, the Frictional force first increase and then decreases with an increase in the Darcy number. For a fixed Frictional force F, it is seen that the volume flow rate $\bar{Q}$ first decreases and then increase with an increase in the Darcy number. The variation of Darcy number has no effect on $\bar{Q}$ for $F = 0$.

In Fig. 7 we have obtained the Frictional force F as a function of the volume flow rate $\bar{Q}$, for different values of τ and for fixed $Da, n, \alpha \; and \; \epsilon$. It is observed that for a given volume flow rate $\bar{Q}$ the Frictional force first decreases and then increase with an increase in the yield stress τ. For a fixed Frictional force, it is seen that the volume flow rate, increase and then decreases, as the yield stress increases. There is no effect of τ on $\bar{Q}$ for $F = 0$ and for $0.3 < \bar{Q} < 0.6$.

The effect of porous thickening ϵ, with fixed values of the other parameters is shown in Fig. 8. For $0 < \bar{Q} < 0.4$, the Frictional force F decreases as ϵ increases and for $\bar{Q} > 0.85$, the Frictional force increases with an increase in the value of ϵ. For a fixed Frictional force F, the volume flow rate $\bar{Q}$ increases in $0 < \bar{Q} < 0.4$ and for $\bar{Q} > 0.85$, it is seen that the volume flow rate decreases as ϵ increases and for $0.4 < \bar{Q} < 0.85$, there is no effect of variation in ϵ.

For fixed values of $Da, \alpha, \epsilon \; and \; \tau$, the effect of the index n is depicted in Fig. 9. It is observed that, for a given volume flow rate $\bar{Q}$ the Frictional force F increases and then decreases with an increase in the index n. And for a fixed Frictional force, it is seen that the volume flow rate $\bar{Q}$ decreases and then increases with an increase in the index number. For $F = 0$, volume flow rate $\bar{Q}$ decreases with an increase in n.

5. Conclusion

Peristaltic transport of a non-Newtonian fluid obeying Herschel–Bulkley fluid properties is investigated under long wave length and low Reynolds number. The expression for pressure rise and frictional force are obtained analytically and the effects of various parameters on the pressure rise and frictional force are studied and depicted graphically.

- In the pumping region, there is a pressure rise with an increase in the yield stress τ and the porous thickening ϵ.
- In the co-pumping region, there is a pressure drop with an increase in the yield stress τ and the porous thickening ϵ.
- In the free pumping region there is no effect of Da and τ on the volume flow rate $\bar{Q}$.
- The frictional force F behaves reversely in comparison with the pressure rise, thus obeying the results of Sobh [7].

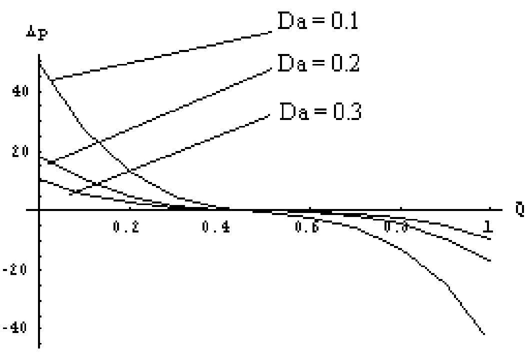

Fig. 2: The variation of pressure Δp with volume flow rate $\bar{Q}$ for different values of Da with $\alpha = 0.1,\ \tau = 0.1,\ \epsilon = 0.3,\ n = 3$.

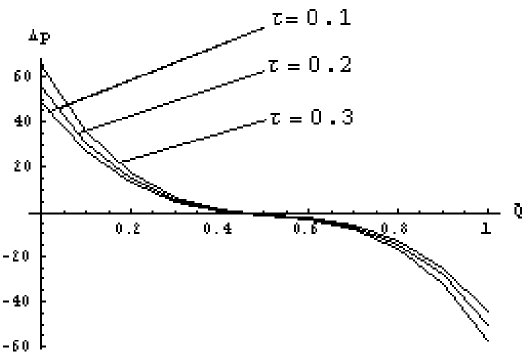

Fig. 3: The variation of pressure Δp with volume flow rate $\bar{Q}$ for different values of τ with $Da = 0.1$, $\alpha = 0.1,\ \epsilon = 0.3,\ n = 3$.

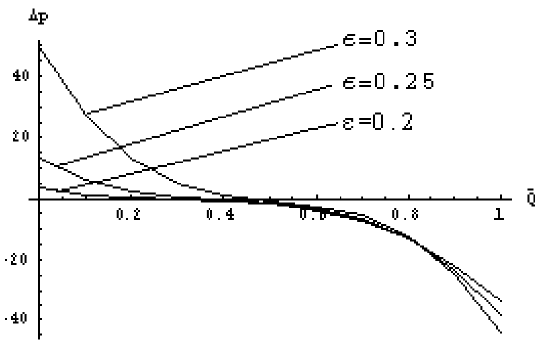

Fig. 4: The variation of pressure Δp with time averaged flux $\bar{Q}$ for different values of ϵ with $Da = 0.1,\ \alpha = 0.1,\ \tau = 0.1,\ n = 3$.

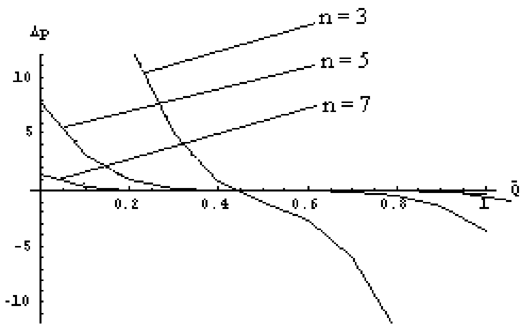

Fig. 5: The variation of pressure Δp with time averaged flux $\bar{Q}$ for different values of n with $Da = 0.1,\ \alpha = 0.1,\ \tau = 0.1,\ \epsilon = 0.3$.

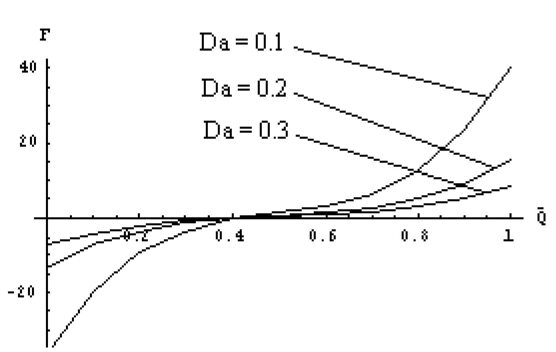

Fig. 6: The variation of Frictional force F with volume flow rate $\bar{Q}$ for different values of Da with $\alpha = 0.1$, $\tau = 0.1$, $\epsilon = 0.3$, $n = 3$.

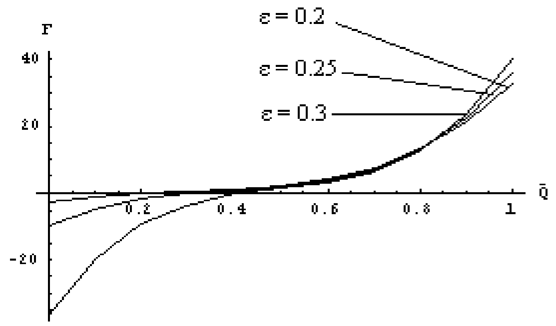

Fig. 8: The variation of Frictional force F with volume flow rate $\bar{Q}$ for different values of ϵ with $Da = 0.1$, $\alpha = 0.1$, $\tau = 0.1$, $n = 3$.

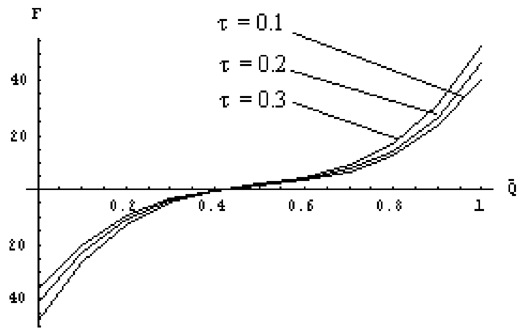

Fig. 7: The variation of Frictional force F with volume flow rate $\bar{Q}$ for different values of τ with $Da = 0.1$, $\alpha = 0.1$, $\epsilon = 0.3$, $n = 3$.

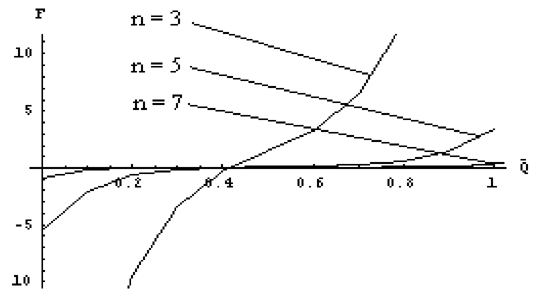

Fig. 9: The variation of Frictional force F with volume flow rate $\bar{Q}$ for different values of n with $Da = 0.1$, $\alpha = 0.1$, $\tau = 0.1$, $\epsilon = 0.3$.

Acknowledgements

The authors are grateful to the referees for their useful comments and suggestions for the improvement of the paper.

References

[1] T.W. Latham, *Fluid motion in peristaltic pumping*, M.S.Thesis, MIT, Cambridge, (1966).

[2] A.H. Shapiro, *Pumping and retrograde diffusion in peristaltic waves, Proc. Workshop in uretral reflux in children*, Nat. Acad. Sci., Washington, D.C., (1967) 109-126.

[3] G.W.Scott Blair, D.C. Spanner, *An Introduction to Biorheology*, Elsevier Science Publishing Company, Amsterdam, Oxford and New York (1974).

[4] H.T. Tang, Y.C. Fung, *Fluid movement in a channel with permeable walls covered by porous media; A model of lung alveolar sheet*, J.Appl.Mech., Volume 97 (1975**)** 45-50.

[5] J.N. Kapur, *Mathematical Models in Biology and Medicine*, Affiliated East–west press Pvt.Lts, New York, (1985).

[6] E.F.El. Shehawey, Kh.S. Mekheimer, S.F. Kalidas and N.A.S. Afifi, *Peristaltic transport through a porous medium*, J.Biomath., Volume 14 (1999).

[7] A. M. Sobh, *Interaction of couple stresses and Slip flow on peristaltic transport in uniform and non uniform channels*, Turkish J. Eng. Sci. Volume 32 (2008) 117-123.

[8] S. Sreenadh, S. Rajendra, S.V.H.N. Krishna Kumari and Y.V.K. Ravi Kumar, *Flow of Herschel Bulkley Fluid in an Inclined Flexible Channel lined with Porous Material Under Peristalsis*, International Journal of Innovative Technology and Creative Engineering ; Volume 1 (2011) 24-31.

[9] M. Kothandapan, J. Prakash, *Influece of heat source, thermal radiation and inclined magnetic field on peristaltic flow of a Hyperbolic tangent nanofluid in a tapered asymmetric channel,*IEEE transactions on Nano Bioscience; Volume 14(4) (2014) 385-392.

[10] M. Ahmed, Abdulhadi, *Effect of wall properties and heat transfer on the peristaltic transport of a Jeffery fluid through porous medium channel,* Mathematical and Theory and Modeling, volume 4 (2014) 86-99.

[11] Nallapu Santhosh and G. Radhakrishnamacharya, *Herschel-Bulkley fluid flow through narrow tubes.* Research Article physics.flu-dyn, 30 Cent. Eur. J. Phys. (2014) 1-12.

[12] Akram Safia and S. Nadeem, *Significance of nanofluid and partial slip on the peristaltic transport of a non-newtonian fluid with different wave forms*, IEEE transactions on nano technology, volume 13 (2014) 375-385.